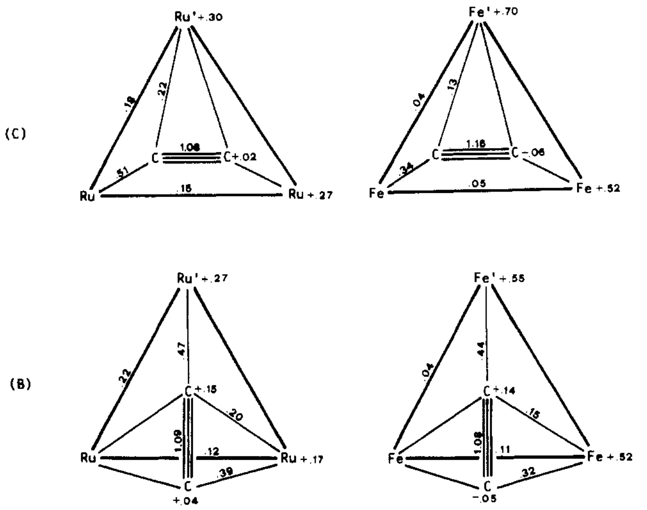

Figure 7. CNDO gross atomic charges and overlap populations of **B** and **C** models of $M_3(CO)_9(HC_2H)$ (M = Fe, Ru) complexes.

values, 1.8 vs. 2.2), which modify the balance between the alkyne–cluster donation/back-donation. In fact, the charge equilibration inside the trimetallic ring in coordination mode **B** for the Fe_3–alkyne complex can be explained by a strong back-donation from the two symmetry-equivalent Fe atoms.[4b,c] On the contrary, in the hypothetical coordination mode **B** for the Ru_3 analogue, the back-donation is not so effective and the charge equilibration is far from being reached; actually, the two equivalent Ru atoms are less positively charged than the unique Ru' atom (see Figure 7). On the other hand, a comparison between the Fe and Ru **C** arrangements (Figure 7) shows that the donation from the alkyne toward the unique metal atom M' is more effective for the Ru than for the Fe compound (larger M'–alkyne OP when M' = Ru). Furthermore, the reduced aptitude of Ru atoms to back-donate is overriden by the favorable geometrical arrangement (compare the Ru atomic charges in **B** and **C**).[38]

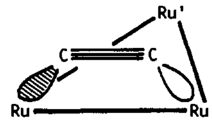

These results suggest that coordination mode **C** could already be favored for a 46-e Ru_3–alkyne compound; the consequent low-lying LUMO would then produce the acquisition of two more electrons in order to reach the 48-e saturated configuration.

Acknowledgments. Thanks are expressed to the Ministero della Pubblica Istruzione (Grant MPI 12/2/15) and to the CNR of Rome for generous financial support of this study. We also thank Johnson-Matthey Ltd. for a loan of $RuCl_3$ and OsO_4. The assistance of a reviewer is acknowledged in the interpretation of the NMR results.

Registry No. **1**, 57373-23-6; **2**, 80303-38-4; **3**, 56943-12-5; **4**, 80303-37-3; **5**, 98797-97-8.

Supplementary Material Available: A table of anisotropic thermal parameters for $H_2Os_3(CO)_9(CH_3C_2CH_3)$ (1 page); a table of structure factor amplitudes for $H_2Os_3(CO)_9(CH_3C_2CH_3)$ (12 pages). Ordering information is given on any current masthead page.

---

(38) A similar bonding scheme has been invoked for the μ_4-η^2 coordination mode **D** of the alkyne in a "butterfly" cluster; actually, the **C** arrangement can be regarded as a portion of a **D** arrangement where a "wing" metal atom has been lost.

Contribution from the Department of Chemistry,
University of South Carolina, Columbia, South Carolina 29208

Ligand Substitution vs. Ligand Addition. 2. Reaction of Dimethylamine with $Ru_3(CO)_9(\mu_3\text{-}S)_2$ and the Crystal and Molecular Structures of $Ru_3(CO)_7(NHMe_2)(\mu\text{-}Me_2NC{=}O)(\mu_3\text{-}S)_2(\mu\text{-}H)$ and $Ru_3(CO)_6(NHMe_2)(\mu\text{-}Me_2NC{=}O)_2(\mu_3\text{-}S)_2$

Richard D. Adams* and James E. Babin

Received June 2, 1986

The reaction of $Ru_3(CO)_9(\mu_3\text{-}S)_2$ (**1**) with an excess of Me_2NH at 25 °C yields two products, $Ru_3(CO)_7(NHMe_2)(\mu\text{-}Me_2NC{=}O)(\mu_3\text{-}S)_2(\mu\text{-}H)$ (**2**, 64%) and $Ru_3(CO)_6(NHMe_2)(\mu\text{-}Me_2NC{=}O)_2(\mu_3\text{-}S)_2$ (**3**, 20%). Both products were characterized by IR and ^1H NMR spectroscopy and elemental and single-crystal X-ray diffraction analyses. For **2**: space group $P2_1/c$, $a = 14.003$ (2) Å, $b = 9.534$ (1) Å, $c = 17.061$ (2) Å, $\beta = 111.91$ (1)°, $Z = 4$, $\rho_{calcd} = 2.14$ g/cm^3. The structure was solved by direct methods and was refined (2816 reflections) to the final values of the residuals $R = 0.0373$ and $R_w = 0.0438$. The structure consists of an open cluster of three metal atoms with two triply bridging sulfido ligands and a C,O-bonded *N,N*-dimethylcarbamoyl ligand bridging an unbonded pair of ruthenium atoms. For **3**: space group $P2_1/c$, $a = 18.030$ (3) Å, $b = 9.148$ (2) Å, $c = 14.397$ (4) Å, $\beta = 90.07$ (2)°, $Z = 4$, $\rho_{calcd} = 2.03$ g/cm^3. The structure was solved by direct methods and was refined (1909 reflections) to the final values of the residuals $R = 0.0497$ and $R_w = 0.0488$. The structure of **3** consists of an open cluster of three metal atoms with only one Ru–Ru bond. There are two triply bridging sulfido ligands, and two *N,N*-dimethylcarbamoyl ligands that bridge both nonbonded Ru–Ru interactions. An intermediate formulated as $Ru_3(CO)_8(NHMe_2)(\mu_3\text{-}S)_2$ was observed spectroscopically when Me_2NH was added to **1** slowly. Reaction of **2** with CO yields $Ru_3(CO)_8(\mu\text{-}Me_2NC{=}O)(\mu_3\text{-}S)_2(\mu\text{-}H)$.

Introduction

Comparitively few studies have been focused on the reactivity of homologous series of transition-metal cluster compounds.[1] In part 1 of this series we reported the results of our studies of the reactions of dimethylamine with the sulfur-bridged trinuclear clusters $M_3(CO)_9(\mu_3\text{-}S)_2$ (M = Fe and Os).[2] It was observed that the iron compound reacted exclusively by a ligand substitution process while the osmium cluster reacted exclusively by an addition reaction, which led to the formation of a bridging carbamoyl ligand that induced the cluster to open. Our studies of the reaction of the third member of this series, $Ru_3(CO)_9(\mu_3\text{-}S)_2$ (**1**), with dimethylamine have now been completed and are described in this report.

Experimental Section

General Procedures. Reactions were performed under a dry nitrogen atmosphere, unless otherwise specified. Reagent grade solvents were

---

(1) Muetterties, E. L.; Burch, R. R.; Stolzenberg, A. M. *Annu. Rev. Phys. Chem.* **1982**, *33*, 89 and references therein.

(2) Adams, R. D.; Babin, J. E. *Inorg. Chem.* **1986**, *25*, 3418.

0020-1669/86/1325-4010$01.50/0

Table I. IR and ^{1}H NMR Spectral Data

compound	IR (ν_{CO}),^{a} cm^{-1}	^{1}H NMR,^{b} δ
$Ru_3(CO)_7(\mu_3\text{-}S)_2(HNMe_2)(\mu\text{-}Me_2NC{=}O)(\mu\text{-}H)$ (**2**)	2095.6 (m), 2033.8 (s), 2029.7 (vs), 2022.9 (m), 2018.2 (w), 1966.0 (m), 1959.4 (w)	3.58 (s, 3 H), 3.05 (s, 3 H), 2.68 (d, 6 H, J_{H-H} = 6.13 Hz), 2.24 (br, 1 H), −11.62 (s, 1 H)
$Ru_3(CO)_6(\mu_3\text{-}S)_2(HNMe_2)(\mu\text{-}Me_2NC{=}O)_2$ (**3**)	2042.9 (vw), 2022.9 (vs), 2016.3 (m), 1959.9 (s), 1961.2 (m), 1946.7 (w)	2.92 (s, 3 H), 2.72 (s, 3 H),^{c} 2.41 (s, 3 H), 2.37 (s, 3 H), 1.94 (d, 3 H, J_{H-H} = 5.93 Hz), 1.86 (d, 3 H, J_{H-H} = 5.91 Hz)
$Ru_3(CO)_8(\mu_3\text{-}S)_2(HNMe_2)$ (**4**)	2084.9 (m), 2049.3 (s), 2026.8 (vs), 2015.6 (s), 2003.5 (vw), 1971.7 (w), 1959.6 (vw)	2.64 (d, 6 H), J_{H-H} = 6.15 Hz)
$Ru_3(CO)_8(\mu_3\text{-}S)_2(\mu\text{-}Me_2NCO{=}O)(\mu\text{-}H)$ (**5**)	2110.7 (w), 2092.1 (vs), 2043.5 (m), 2036.8 (vs), 2030.0 (s), 2012.9 (w), 1973.9 (m)	3.60 (s, 3 H), 3.06 (s, 3 H), −11.09 (s, 1 H)

^{a}Hexane solvent. ^{b}$CDCl_3$ solvent. ^{c}C_6D_6 solvent.

dried over molecular sieves and deoxygenated by purging with N_2 prior to use. Dimethylamine and CP grade CO gases were obtained from Linde Corp. and were used without further purification. $Ru_3(CO)_{12}$ was used as purchased from Strem Chemicals, Newburyport, MA. Ethylene sulfide was purchased from Aldrich and was used without further purification. IR spectra were recorded on a Nicolet 5DXB FT IR spectrophotometer. A Bruker AM300 FT-NMR spectrometer was used to obtain ^{1}H NMR spectra. Elemental microanalyses were performed by MICANAL, Tucson, AZ.

Preparation of $Ru_3(CO)_9(\mu_3\text{-}S)_2$ (1). 200-mg (0.323-mmol) sample of $Ru_3(CO)_{12}$ was dissolved in 100 mL of cyclohexane solvent. A 93-μL (1.615-mmol) aliquot of ethylene sulfide was added to the solution via syringe, and the resulting mixture was refluxed for 1 h in the presence of a slow purge with CO. The solvent was removed in vacuo, and the residue was extracted with a small amount of hexane. Purification was obtained by column chromatography over Florisil with hexane solvent. Yield of $Ru_3(CO)_9(\mu_3\text{-}S)_2$ (**1**): 182 mg (91%). This compound is spectroscopically idential with its formula equivalent obtained from the reaction of $Ru_3(CO)_{12}$ with elemental sulfur.[3]

Reactions of 1 with Me_2NH. (a) With Excess Dimethylamine. Dimethylamine was bubbled through a solution of **1** (50 mg, 0.0807 mmole) in 40 mL of CH_2Cl_2 for 2 min at 25 °C. The solvent was removed in vacuo from the orange solution, and the residue was chromatographed on silica gel TLC plates. Elution with a 45%/55% CH_2Cl_2/hexane solution separated in order of elution $Ru_3(CO)_7(NHMe_2)(\mu\text{-}Me_2NC{=}O)(\mu_3\text{-}S)_2$ (μ-H) (**2**, 32 mg (64%)) and $Ru_3(CO)_6(MHMe_2)(\mu\text{-}Me_2NC{=}O)_2(\mu_3\text{-}S)_2$ (**3**, 10.2 mg (20%)). Anal. Calcd for **2**: C, 21.15; N, 4.11; H, 2.07. Found: C, 21.20; N, 4.06; H, 1.88; Calcd for **3**: C, 23.20; N, 5.80; H, 2.62. Found: C, 23.19; N, 5.59; H, 2.56. IR and NMR spectral data are listed in Table I.

(b) By Slow Addition of Me_2NH. A 5-cm^3 sample of gaseous dimethylamine was added from a syringe to a solution of **1** (30 mg, 0.0484 mmol) in 50 mL of hexane, and the course of the reaction was followed by IR spectroscopy. After 8 h at 25 °C, prominent absorptions were observed at 2085, 2049, 2027, 2016, 2004, 1972, and 1960 cm^{-1}. Efforts to isolate this species have been unsuccessful, but on the basis of a spectroscopic comparison with the known compound $Fe_3(CO)_8(NHMe_2)(\mu_3\text{-}S)_2$, it is believed to be $Ru_3(CO)_8(NHMe_2)(\mu_3\text{-}S)_2$ (**4**). At this time an additional 10 cm^3 of Me_2NH gas was added to the reaction flask. The IR spectrum began to change, and after an additional 18 h, it was very similar to that of compound **2**. Finally, a third 10-cm^3 portion of Me_2NH was added to the flask, and after 19 h more, the IR spectrum was essentially identical with that of compound **3**. A similar sequence of transformations was observed by performing the reaction in an NMR tube and monitoring by ^{1}H NMR spectroscopy.

Reaction of 2 with CO. 20-mg (0.0294-mmol) sample of **2** was dissolved in 40 mL of hexane, and the solution was refluxed under an atmosphere of CO for 5 h. After removal of the solvent in vacuo, the residue was extracted with a minimum quantity of CH_2Cl_2 and was chromatographed by TLC on silica gel coated plates. Elution with a 20%/80% CH_2Cl_2/hexane solution led to the isolation of $Ru_3(CO)_8(\mu\text{-}Me_2NC{=}O)(\mu_3\text{-}S)_2(\mu\text{-}H)$ (**5**, 8.2 mg (46%)). Anal. Calcd for **5**: C, 19.88; N, 2.11; H, 1.06. Found: C, 19.87; N, 2.14; H, 0.96. IR and NMR spectra for **5** are listed in Table I.

Crystallographic Analyses. Orange crystals of **2** were obtained by slow evaporation of CH_2Cl_2/hexane solutions at −20 °C. Orange crystals of **3** were grown by slow evaporation of hexane solutions at 25 °C. All crystals were mounted in thin-walled glass capillaries. Diffraction measurements were made on a Rigaku AFC6 fully automated four-circle diffractometer using graphite monochromatized Mo Kα radiation. Unit cells were detd. and refined from 25 randomly selected reflections obtained by using the automatic search, center, index, and least-squares routines. Crystal data, data collection parameters, and results of the analyses are listed in Table II. All data processing was performed on a Digital Equipment Corp. MICROVAX I computer by using the TEXSAN structure solving program library obtained from the Molecular Structure Corp., College Station, TX. Neutral-atom scattering factors were calculated by the standard procedures.[4a] Anomalous dispersion corrections were applied to all non-hydrogen atoms.[4b] Full-matrix least-squares refinements minimized the function

$$\sum_{hkl} w(|F_o| - |F_c|)^2$$

where $w = 1/\sigma(F)^2$, $\sigma(F) = \sigma(F_o^2)/2F_o$ and $\sigma(F_o^2) = [\sigma(I_{raw})^2 + (PF_o^2)^2]^{1/2}/Lp$.

Both compounds crystallized in the monoclinic crystal system. Space group $P2_1/c$ was identified for both structures on the basis of the systematic absences observed during the collection of data. The coordinates of the heavy atoms in both structures were obtained by direct methods (MULTAN). All remaining non-hydrogen atoms were subsequently obtained from difference Fourier syntheses. In both structures the coordination of the hydrogen atom bonded to the nitrogen atom in the dimethylamine ligand were obtained from a difference Fourier synthesis; however, the positions of the methyl hydrogen atoms were calculated by assuming idealized tetrahedral and staggered conformational geometries. The contributions of all hydrogen atoms were added to the structure factor calculations, but their positions were not refined. Error analyses were calculated from the inverse matrix obtained on the final cycle of refinement for each structure. See the supplementary material for the tables of structure factor amplitudes and anisotropic thermal parameters.

Results

When $Ru_3(CO)_9(\mu_3\text{-}S)_2$ (**1**) was allowed to react with an excess of Me_2NH in CH_2Cl_2 solvent at 25 °C for 2 min., two major products were formed. These were isolated and identified as $Ru_3(CO)_7(NHMe_2)(\mu\text{-}Me_2NC{=}O)(\mu_3\text{-}S)_2(\mu\text{-}H)$ (**2**, 64% yield) and $Ru_3(CO)_6(\mu\text{-}Me_2NC{=}O)_2(\mu_3\text{-}S)_2$ (**3**, 20% yield). Both products were characterized by IR and ^{1}H NMR spectroscopy and elemental and single-crystal X-ray diffraction analyses. IR and ^{1}H NMR spectra are listed in Table I. Atomic positional parameters, interatomic distances and angles for the structural analysis of compound **2** are given in Tables III–V, respectively. An ORTEP drawing of the molecular structure of **2** is shown in Figure 1. The molecule consists of an open cluster of three ruthenium atoms. Only one distance, Ru(1)–Ru(2) = 2.7715 (9) Å is short enough to allow for a significant metal–metal interaction. Compound **2** contains a hydride ligand (δ = 11.62) that was not located crystallographically, but is believed to bridge the Ru(1)–Ru(2) bond in the cavity circumscribed by the carbonyl

---

[3] Johnson, B. F. G.; Lewis, J.; Lodge, P. G.; Raithby, P. R.; Henrick, K.; McPartlin, M. *J. Chem. Soc., Chem. Commun.* **1979**, 719.

[4] *International Tables X-ray Crystallography*; Kynoch: Birmingham, England, 1975; Vol. IV: (a) Table 2.2B, pp 99–101; (b) Table 2.3.1, 149–150.

Table II. Crystallographic Data for X-ray Diffraction Studies

	2	**3**
	(A) Crystal Data	
formula	$Ru_3S_2O_8N_2C_{12}H_{14}$	$Ru_3S_2O_8N_3C_{14}H_{19}$
temp, °C	23 (±3)	23 (±3)
space group	$P2_1/c$, No. 14	$P2_1/c$, No. 14
a, Å	14.003 (2)	18.030 (3)
b, Å	9.534 (1)	9.148 (2)
c, Å	17.061 (2)	14.397 (4)
β, deg	111.91 (1)	90.07 (2)
V, Å^3	2113.0	2374.5
M_r	681.5	724.5
Z	4	4
ρ_{calcd}, g/cm^3	2.14	2.03
	(B) Measurement of Intensity Data	
radiation	Mo Kα (0.71073 Å)	Mo Kα (0.71073 Å)
monochromator	graphite	graphite
detector aperture, mm		
horiz	2.0	2.0
vert	2.0	2.0
cryst faces	$101, 10\bar{1}, 100, \bar{1}00, 0\bar{2}1, \bar{1}20$	$100, \bar{1}00, 001, 00\bar{1}, 010, 0\bar{1}0$
cryst size, mm	0.11 × 0.46 × 0.12	0.24 × 0.13 × 0.03
cryst orientation		
direction; deg from ϕ axis	b; 6.6	b; 6.3
reflcns measd	$h,k,\pm l$	$h,k,\pm l$
max 2θ, deg	50	50
scan type	moving cryst–stationary counter	moving cryst–stationary counter
ω-scan width: $(A + 0.347 \tan \theta)°$	$A = 1.10$	$A = 1.10$
bkgd (count time, at each end of scan), s	3.0	3.0
ω-scan rate,[a] deg/min	4.0	4.0
no. f reflcns measd	4112	4619
no. of data used ($F^2 \geq 3.0\sigma(F^2)$)	2816	1909
	(C) Treatment of Data	
abs cor	none applied	none applied
coeff, cm^{-1}	22.9	20.5
no. of variables (refined)	244	271
P factor	0.03	0.03
final residuals		
R_F	0.0373	0.0497
R_{wF}	0.0438	0.0488
esd. of unit wt observn	1.62	1.26
largest shift/error value of final cycle	0.00	0.00
largest peak in final diff Fourier, e/Å^3	1.0	0.9

[a] Rigaku software uses a multiple scan technique. If the $I/\sigma(I)$ ratio is less than 10.0, a second scan is made and the results are added to first scan, etc. A maximum of three scans was permitted per reflection.

Table III. Positional Parameters and B(eq) for $Ru_3(CO)_7(NHMe_2)(\mu\text{-}Me_2NC{=}O)(\mu_3\text{-}S)_2(\mu\text{-}H)$ (**2**)

atom	x	y	z	B(eq), Å^2
Ru(1)	0.688108 (47)	0.758455 (62)	1.004222 (36)	3.7
Ru(2)	0.846145 (43)	0.762481 (58)	0.943523 (37)	3.4
Ru(3)	0.663992 (41)	0.969341 (60)	0.819586 (34)	3.2
S(1)	0.76283 (13)	0.97061 (18)	0.97086 (10)	2.7
S(2)	0.66563 (13)	0.72617 (19)	0.85693 (11)	2.8
O	0.80194 (35)	0.93648 (49)	0.79827 (29)	3.8
O(11)	0.76858 (49)	0.85583 (72)	1.18768 (37)	6.0
O(12)	0.65958 (58)	0.44928 (66)	1.03238 (42)	7.8
O(13)	0.46523 (45)	0.83362 (70)	0.97592 (38)	5.9
O(21)	1.04680 (44)	0.83584 (66)	1.08347 (40)	4.5
O(22)	0.90389 (55)	0.47522 (64)	0.90297 (49)	7.2
O(31)	0.54142 (44)	0.92772 (80)	0.63315 (34)	5.5
O(33)	0.46783 (40)	1.03749 (67)	0.84170 (35)	6.3
N	0.95789 (46)	0.84984 (71)	0.82559 (42)	4.5
N(1)	0.70792 (45)	1.18645 (62)	0.81220 (38)	3.8
C	0.87428 (53)	0.85813 (73)	0.84653 (44)	3.0
C(1)	1.04990 (64)	0.77202 (95)	0.87349 (59)	5.4
C(2)	0.96242 (69)	0.9276 (12)	0.75423 (63)	7.5
C(3)	0.7125 (11)	1.2313 (10)	0.73031 (72)	8.8
C(4)	0.65857 (87)	1.28890 (95)	0.84472 (80)	9.3
C(11)	0.73774 (61)	0.81545 (86)	1.12184 (50)	4.4
C(12)	0.66492 (67)	0.56412 (94)	1.02203 (61)	5.0
C(13)	0.54746 (64)	0.81204 (88)	0.98411 (46)	4.0
C(21)	0.97380 (58)	0.80837 (76)	1.02914 (50)	3.8
C(22)	0.88398 (60)	0.58422 (90)	0.91946 (64)	4.4
C(31)	0.58855 (57)	0.94548 (87)	0.70259 (50)	4.4
C(33)	0.54286 (57)	1.00981 (79)	0.83362 (43)	3.5

Table IV. Intramolecular Distances for $Ru_3(CO)_7(NHMe_2)(\mu\text{-}Me_2NC{=}O)(\mu_3\text{-}S)_2(H)$ (**2**)[a]

Ru(1)–C(12)	1.925 (9)	Ru(3)–S(2)	2.402 (2)
Ru(1)–C(13)	1.937 (9)	Ru(3)–S(1)	2.431 (2)
Ru(1)–C(11)	1.940 (8)	O–C	1.280 (8)
Ru(1)–S(2)	2.433 (2)	O(11)–C(11)	1.111 (9)
Ru(1)–S(1)	2.440 (2)	O(12)–C(12)	1.12 (1)
Ru(1)–Ru(2)	2.7715 (9)	O(13)–C(13)	1.126 (9)
Ru(2)–C(22)	1.871 (9)	O(21)–C(21)	1.125 (9)
Ru(2)–C(21)	1.890 (8)	O(22)–C(22)	1.14 (1)
Ru(2)–C	2.052 (7)	O(31)–C(31)	1.133 (9)
Ru(2)–S(2)	2.430 (2)	O(33)–C(33)	1.140 (8)
Ru(2)–S(1)	2.433 (2)	N–C	1.348 (9)
Ru(3)–C(33)	1.840 (8)	N–C(1)	1.45 (1)
Ru(3)–C(31)	1.892 (8)	N–C(2)	1.45 (1)
Ru(3)–O	2.118 (4)	N(1)–C(4)	1.42 (1)
Ru(3)–N(1)	2.176 (6)	N(1)–C(3)	1.49 (1)
Ru(1)···Ru(3)	3.645 (1)	Ru(2)···Ru(3)	3.293 (1)

[a] Distances are in angstroms. Estimated standard deviations in the least significant figure are given in parentheses.

ligands C(11)–O(11), C(12)–O(12), C(21)–O(21), and C(22)–O(22). The Ru(1)–Ru(2) distances is approximately 0.1 Å shorter than the hydride-bridged Ru–Ru distances found in $Ru_3(CO)_9(\mu_3\text{-}S)(\mu\text{-}H)_2$.[5] The Ru(1)–Ru(3) and Ru(2)–Ru(3) distances of 3.645 (1) and 3.293 (1) Å, respectively, are in the nonbonding range. There are two triply bridging sulfido ligands symmetrically disposed about the triruthenium plane. The metal–sulfur distances span a narrow range of 2.402 (2)–2.440 (2) Å. They are slightly longer than those observed in the closed cluster $Ru_3(CO)_9(\mu_3\text{-}S)(\mu\text{-}H)_2$[5] but are similar in length to those observed in the open cluster $Ru_3(CO)_8(SnCl_3)(\mu\text{-}Cl)(\mu_3\text{-}S)(\mu\text{-}H)_2$.[5] The dimethylamine ligand is coordinated to Ru(3); Ru(3)–N(1) = 2.176 (6) Å. An *N,N*-dimethylcarbamoyl ligand bridges the metal atoms Ru(2) and Ru(3); Ru(2)–C = 2.052 (7) Å, and Ru(3)–O = 2.118 (4) Å. These distances are similar to those of 2.098 (8) and 2.100 (5) Å found to the bridging dimethylcarbamoyl ligand in $Ru_3(CO)_{10}(\mu\text{-}Me_2NC{=}O)(\mu\text{-}H)$.[6] The C–O bond is double in character, 1.280 (8) Å, and partial multiple bonding exists between the C and N atoms, 1.348 (9) Å. These distances are similar to those found for bridging carbamoyl ligands in other cluster complexes.[2,6-8] The nitrogen atom is planar, and there is a hindered rotation about the C-N bond since separate resonances are observed for the carbamoyl *N*-methyl groups. According to the structural analysis, the methyl groups on the Me_2NH ligand are also inequvalent; however, only a single resonance (coupled to the NH proton) is observed. This could be explained by an averaging process through which the amine ligand interchanges sites with the carbonyl ligand C(31)–O(31). Variable-temperature NMR studies to confirm the existence of such an exchange process were not performed.

---

(5) Adams, R. D.; Katahira, D. A. *Organometallic* **1982**, *1*, 53.

(6) Szostak, R.; Strouse, C. E.; Kaesz, H. D. *J. Organomet. Chem.* **1980**, *191*, 243.

(7) Adams, R. D.; Golembeski, N. M.; Selegue, J. *Inorg. Chem.* **1981**, *20*, 1242.

(8) Boag, N. M.; Knobler, C. B.; Kaesz, H. D. *Angew. Chem., Int. Ed. Engl.* **1983**, *22*, 249.

Table V. Intramolecular Bond Angles for $Ru_3(CO)_7(NHMe_2)(\mu\text{-}Me_2NC{=}O)(\mu_3\text{-}S)_2(H)$ (**2**)[a]

C(12)–Ru(1)–C(13)	93.5 (4)	C(33)–Ru(3)–S(1)	92.8 (2)
C(12)–Ru(1)–C(11)	97.0 (3)	C(31)–Ru(3)–O	89.3 (2)
C(12)–Ru(1)–S(2)	94.4 (2)	C(31)–Ru(3)–N(1)	96.4 (3)
C(12)–Ru(1)–S(1)	161.3 (3)	C(31)–Ru(3)–S(2)	96.3 (3)
C(12)–Ru(1)–Ru(2)	106.1 (2)	C(31)–Ru(3)–S(1)	173.4 (3)
C(13)–Ru(1)–C(11)	93.3 (3)	O–Ru(3)–N(1)	80.5 (2)
C(13)–Ru(1)–S(2)	96.8 (2)	O–Ru(3)–S(2)	89.1 (1)
C(13)–Ru(1)–S(1)	103.7 (2)	O–Ru(3)–S(1)	89.3 (1)
C(13)–Ru(1)–Ru(2)	146.2 (2)	N(1)–Ru(3)–S(2)	163.4 (2)
C(11)–Ru(1)–S(2)	164.2 (2)	N(1)–Ru(3)–S(1)	89.7 (2)
C(11)–Ru(1)–S(1)	89.4 (2)	S(2)–Ru(3)–S(1)	77.17 (6)
C(11)–Ru(1)–Ru(2)	110.8 (2)	Ru(3)–S(1)–Ru(2)	85.20 (6)
S(2)–Ru(1)–S(1)	76.43 (6)	Ru(3)–S(1)–Ru(1)	96.87 (6)
S(2)–Ru(1)–Ru(2)	55.21 (5)	Ru(2)–S(1)–Ru(1)	69.32 (5)
S(1)–Ru(1)–Ru(2)	55.23 (4)	Ru(3)–S(2)–Ru(2)	85.90 (6)
C(22)–Ru(2)–C(21)	96.7 (3)	Ru(3)–S(2)–Ru(1)	97.85 (7)
C(22)–Ru(2)–C	94.1 (3)	Ru(2)–S(2)–Ru(1)	69.49 (5)
C(22)–Ru(2)–S(2)	93.0 (2)	C–O–Ru(3)	122.0 (4)
C(22)–Ru(2)–S(1)	168.0 (2)	C–N–C(1)	124.0 (7)
C(22)–Ru(2)–Ru(1)	113.6 (3)	C–N–C(2)	120.5 (7)
C(21)–Ru(2)–C	96.3 (3)	C(1)–N–C(2)	115.4 (7)
C(21)–Ru(2)–S(2)	166.5 (2)	C(4)–N(1)–C(3)	111.5 (7)
C(21)–Ru(2)–S(1)	92.6 (2)	C(4)–N(1)–Ru(3)	116.2 (5)
C(21)–Ru(2)–Ru(1)	111.8 (2)	C(3)–N(1)–Ru(3)	116.2 (5)
C–Ru(2)–S(2)	92.4 (2)	O–C–N	114.9 (7)
C–Ru(2)–S(1)	92.4 (2)	O–C–Ru(2)	115.7 (5)
C–Ru(2)–Ru(1)	136.7 (2)	N–C–Ru(2)	129.4 (6)
S(2)–Ru(2)–S(1)	76.60 (6)	O(11)–C(11)–Ru(1)	175.4 (8)
S(2)–Ru(2)–Ru(1)	55.30 (5)	O(12)–C(12)–Ru(1)	174.1 (8)
S(1)–Ru(2)–Ru(1)	55.46 (4)	O(13)–C(13)–Ru(1)	174.4 (7)
C(33)–Ru(3)–C(31)	89.1 (3)	O(21)–C(21)–Ru(2)	175.8 (8)
C(33)–Ru(3)–O	175.8 (3)	O(22)–C(22)–Ru(2)	177.8 (8)
C(33)–Ru(3)–N(1)	95.9 (3)	O(31)–C(31)–Ru(3)	177.6 (7)
C(33)–Ru(3)–S(2)	94.9 (2)	O(33)–C(33)–Ru(3)	178.6 (7)

[a] Angles are in degrees. Estimated standard deviations in the least significant figure are given in parentheses.

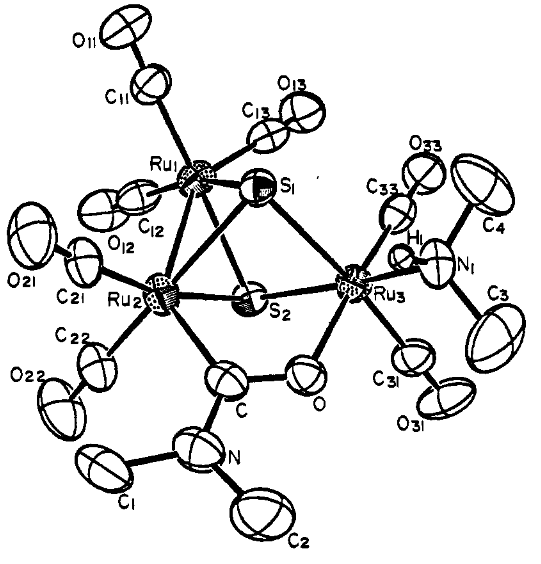

Figure 1. ORTEP diagram of $Ru_3(CO)_7(NHMe_2)(\mu\text{-}Me_2NC{=}O)(\mu_3\text{-}S)_2(\mu\text{-}H)$ (**2**), showing 50% probability thermal ellipsoids. The hydrogen atom H(1) is shown with an artificially reduced thermal ellipsoid. The other hydrogen atoms are not shown.

Table VI. Positional Parameters and *B*(eq) for $Ru_3(CO)_6(NHMe_2)(\mu\text{-}Me_2NC{=}O)_2(\mu_3\text{-}S)_2$ (**3**)

atom	*x*	*y*	*z*	*B*(eq), Å^2
Ru(1)	0.800 177 (67)	−0.109 43 (14)	0.992 131 (84)	3.01 (6)
Ru(2)	0.666 696 (67)	0.115 23 (15)	0.951 115 (90)	3.27 (6)
Ru(3)	0.844 716 (68)	0.155 11 (14)	0.894 617 (86)	2.81 (6)
S(1)	0.749 54 (22)	−0.019 40 (43)	0.849 04 (28)	3.2 (2)
S(2)	0.780 15 (20)	0.138 15 (43)	1.039 33 (26)	3.2 (2)
O(1)	0.765 98 (55)	0.312 4 (11)	0.860 08 (68)	3.5 (5)
O(2)	0.649 42 (54)	−0.095 9 (12)	1.024 68 (74)	4.0 (6)
O(11)	0.884 67 (77)	−0.183 8 (14)	1.167 86 (88)	6.6 (8)
O(12)	0.857 51 (82)	−0.374 8 (15)	0.893 58 (96)	7.2 (9)
O(21)	0.536 10 (76)	0.042 3 (18)	0.828 0 (11)	8 (1)
O(22)	0.577 48 (78)	0.267 3 (16)	1.098 29 (98)	7.4 (9)
O(31)	0.958 01 (67)	0.370 0 (15)	0.967 11 (83)	6.4 (8)
O(33)	0.971 95 (64)	−0.053 8 (14)	0.910 30 (80)	5.3 (7)
N(1)	0.654 93 (71)	0.406 0 (16)	0.844 85 (92)	4.5 (7)
N(2)	0.684 35 (77)	−0.317 6 (15)	1.072 51 (95)	4.4 (8)
N(3)	0.874 04 (65)	0.187 6 (15)	0.748 98 (84)	3.7 (7)
C(1)	0.698 23 (87)	0.296 0 (17)	0.878 7 (11)	3.4 (8)
C(2)	0.701 69 (93)	−0.188 3 (18)	1.034 7 (10)	3.7 (8)
C(3)	0.684 30 (97)	0.523 6 (19)	0.788 2 (14)	6 (1)
C(4)	0.575 07 (96)	0.416 5 (22)	0.856 5 (13)	6 (1)
C(5)	0.734 9 (10)	−0.437 9 (20)	1.082 4 (13)	5 (1)
C(6)	0.606 2 (11)	−0.339 0 (21)	1.102 0 (15)	7 (1)
C(7)	0.912 05 (96)	0.322 4 (19)	0.727 8 (13)	5 (1)
C(8)	0.908 7 (11)	0.062 6 (25)	0.701 3 (14)	7 (1)
C(11)	0.850 88 (91)	−0.154 2 (20)	1.103 0 (12)	4 (1)
C(12)	0.830 04 (95)	−0.276 2 (21)	0.930 6 (12)	4 (1)
C(21)	0.583 23 (96)	0.071 5 (21)	0.872 6 (13)	5 (1)
C(22)	0.609 64 (96)	0.213 4 (20)	1.040 4 (14)	5 (1)
C(31)	0.913 81 (92)	0.294 3 (17)	0.941 5 (11)	3.5 (8)
C(33)	0.919 29 (91)	0.017 7 (17)	0.909 2 (10)	3.4 (8)

Table VII. Intramolecular Distances for $Ru_3(CO)_6(NHMe_2)(\mu\text{-}Me_2NC{=}O)_2(\mu_3\text{-}S)_2$ (**3**)[a]

Ru(1)–C(12)	1.85 (2)	Ru(3)–S(1)	2.433 (4)
Ru(1)–C(11)	1.88 (2)	O(1)–C(1)	1.26 (2)
Ru(1)–C(2)	2.01 (2)	O(2)–C(2)	1.27 (2)
Ru(1)–S(2)	2.392 (4)	O(11)–C(11)	1.15 (2)
Ru(1)–S(1)	2.398 (4)	O(12)–C(12)	1.16 (2)
Ru(1)–Ru(3)	2.911 (2)	O(21)–C(21)	1.10 (2)
Ru(2)–C(22)	1.88 (2)	O(22)–C(22)	1.13 (2)
Ru(2)–C(21)	1.92 (2)	O(31)–C(31)	1.12 (2)
Ru(2)–C(1)	2.04 (2)	O(33)–C(33)	1.15 (2)
Ru(2)–O(2)	2.22 (1)	N(1)–C(1)	1.36 (2)
Ru(2)–S(2)	2.416 (4)	N(1)–C(3)	1.45 (2)
Ru(2)–S(1)	2.432 (4)	N(1)–C(4)	1.45 (2)
Ru(3)–C(33)	1.85 (2)	N(2)–C(2)	1.34 (2)
Ru(3)–C(31)	1.90 (2)	N(2)–C(5)	1.43 (2)
Ru(3)–O(1)	2.08 (1)	N(2)–C(6)	1.49 (2)
Ru(3)–N(3)	2.18 (1)	N(3)–C(7)	1.44 (2)
Ru(3)–S(2)	2.393 (4)	N(3)–C(8)	1.47 (2)
Ru(1)–Ru(2)	3.219 (1)	Ru(2)–Ru(3)	3.332 (1)
Ru(1)–C(33)	2.72 (2)		

[a] Distances are in angstroms. Estimated standard deviations in the least significant figure are given in parentheses.

Atomic positional parameters and interatomic distances and angles for the structural analysis of compound **3** are given in Tables VI–VIII. An ORTEP drawing of the molecular structure of **3** is shown in Figure 2. The molecule consists of an open cluster of three metal atoms that is similar to that of **2**. There is one metal–metal bond, Ru(1)–Ru(3) = 2.911 (2) Å. The two nonbonding contacts are Ru(1)–Ru(2) = 3.219 (1) Å and Ru(2)–Ru(3) = 3.332 (1) Å. There are two triply bridging sulfido ligands located symmetrically on opposite sides of the triruthenium plane. The ruthenium–sulfur distances are very similar to those in **2**. There are two C,O-bonded bridging *N,N*-dimethylcarbamoyl ligands, one across each of the nonbonded Ru–Ru atomic pairs. One ligand C-bonded to Ru(2) while the other is O-bonded to Ru(2). The Ru(1)–C(2) and Ru(2)–C(1) distances of 2.01 (2) and 2.04 (2) Å was similar to each other and to those observed in **2** and in $Ru_3(CO)_{10}(\mu\text{-}Me_2NC{=}O)(\mu\text{-}H)$.[6] The Ru(3)–O(1) distance at 2.08 (1) Å is similar to that in **2** and in $Ru_3(CO)_{10}(\mu\text{-}Me_2NC{=}O)(\mu\text{-}H)$, but the Ru(2)–O(2) distance of 2.22 (1) Å is significantly longer than all the others. Since the Ru(2)–O(2) bond is trans to the Ru(2)–C(1) bond, C(1)–Ru(2)–O(2) = 171.2 (5)°, the Ru(2)–O(2) lengthening could be due to a strong trans influence of the carbamoyl carbon C(1). The carbamoyl C–O distances are equal within experimental error, 1.26 (2) and 1.27 (2) Å, as are C–N distances, 1.36 (2) and 1.34 (2) Å. A dimethylamine ligand is coordinated to Ru(3). The Ru(3)–N(3) distance of 2.18 (1) Å is essentially identical with the Ru–N distance to the amine ligand in **2**. Each ruthenium atom contains

Table VIII. Intramolecular Bond Angles for $Ru_3(CO)_6(NHMe_2)(\mu\text{-}Me_2NC{=}O)_2(\mu_3\text{-}S)_2$ (**3**)[a]

C(12)–Ru(1)–C(11)	94.9 (7)	O(1)–Ru(3)–N(3)	80.9 (4)
C(12)–Ru(1)–C(2)	96.2 (7)	O(1)–Ru(3)–S(2)	85.4 (3)
C(12)–Ru(1)–S(2)	164.5 (6)	O(1)–Ru(3)–S(1)	84.7 (3)
C(12)–Ru(1)–S(1)	89.0 (5)	O(1)–Ru(3)–Ru(1)	120.1 (3)
C(12)–Ru(1)–Ru(3)	112.0 (5)	N(3)–Ru(3)–S(2)	164.5 (3)
C(11)–Ru(1)–C(2)	95.2 (7)	N(3)–Ru(3)–S(1)	90.1 (3)
C(11)–Ru(1)–S(2)	92.2 (5)	N(3)–Ru(3)–Ru(1)	130.1 (4)
C(11)–Ru(1)–S(1)	170.6 (5)	S(2)–Ru(3)–S(1)	81.3 (1)
C(11)–Ru(1)–Ru(3)	117.1 (5)	S(2)–Ru(3)–Ru(1)	52.5 (1)
C(2)–Ru(1)–S(2)	96.9 (5)	S(1)–Ru(3)–Ru(1)	52.4 (1)
C(2)–Ru(1)–S(1)	92.8 (5)	Ru(1)–S(1)–Ru(2)	83.6 (1)
C(2)–Ru(1)–Ru(3)	133.5 (5)	Ru(1)–S(1)–Ru(2)	83.6 (1)
S(2)–Ru(1)–S(1)	82.0 (1)	Ru(1)–S(1)–Ru(3)	74.1 (1)
S(2)–Ru(1)–Ru(3)	52.5 (1)	Ru(2)–S(1)–Ru(3)	86.5 (1)
S(1)–Ru(1)–Ru(3)	53.5 (1)	Ru(1)–S(2)–Ru(3)	74.9 (1)
C(22)–Ru(2)–C(21)	94.2 (8)	Ru(1)–S(2)–Ru(2)	84.1 (1)
C(22)–Ru(2)–C(1)	96.6 (7)	Ru(3)–S(2)–Ru(2)	87.7 (1)
C(22)–Ru(2)–O(2)	90.7 (6)	C(1)–O(1)–Ru(3)	122 (1)
C(22)–Ru(2)–S(2)	93.6 (6)	C(2)–O(2)–Ru(2)	122 (1)
C(22)–Ru(2)–S(1)	173.8 (6)	C(1)–N(1)–C(3)	123 (1)
C(21)–Ru(2)–C(1)	95.0 (7)	C(1)–N(1)–C(4)	125 (1)
C(21)–Ru(2)–O(2)	89.4 (6)	C(3)–N(1)–C(4)	112 (1)
C(21)–Ru(2)–S(2)	171.4 (5)	C(2)–N(2)–C(5)	125 (1)
C(21)–Ru(2)–S(1)	91.2 (5)	C(2)–N(2)–C(6)	117 (2)
C(1)–Ru(2)–O(2)	171.2 (5)	C(5)–N(2)–C(6)	118 (1)
C(1)–Ru(2)–S(2)	87.8 (4)	C(7)–N(3)–C(8)	111 (1)
C(1)–Ru(2)–S(1)	86.0 (4)	C(7)–N(3)–Ru(3)	116 (1)
O(2)–Ru(2)–S(2)	86.8 (3)	C(8)–N(3)–Ru(3)	116 (1)
O(2)–Ru(2)–S(1)	86.2 (3)	O(1)–C(1)–N(1)	113 (1)
S(2)–Ru(2)–S(1)	80.9 (1)	O(1)–C(1)–Ru(2)	118 (1)
C(33)–Ru(3)–C(31)	86.5 (7)	N(1)–C(1)–Ru(2)	128 (1)
C(33)–Ru(3)–O(1)	172.4 (5)	O(2)–C(2)–N(2)	117 (1)
C(33)–Ru(3)–N(3)	91.4 (6)	O(2)–C(2)–Ru(1)	112 (1)
C(33)–Ru(3)–S(2)	102.2 (5)	N(2)–C(2)–Ru(1)	130 (1)
C(33)–Ru(3)–S(1)	95.6 (5)	O(11)–C(11)–Ru(1)	177 (2)
C(33)–Ru(3)–Ru(1)	65.3 (5)	O(12)–C(12)–Ru(1)	172 (2)
C(31)–Ru(3)–O(1)	93.9 (6)	O(21)–C(21)–Ru(2)	178 (2)
C(31)–Ru(3)–N(3)	95.2 (6)	O(22)–C(22)–Ru(2)	176 (2)
C(31)–Ru(3)–S(2)	93.1 (5)	O(31)–C(31)–Ru(3)	175 (2)
C(31)–Ru(3)–S(1)	174.3 (5)	O(33)–C(33)–Ru(3)	170 (1)
C(31)–Ru(3)–Ru(1)	124.5 (5)		

[a] Angles are in degrees. Estimated standard deviations in the least significant figure are given in parentheses.

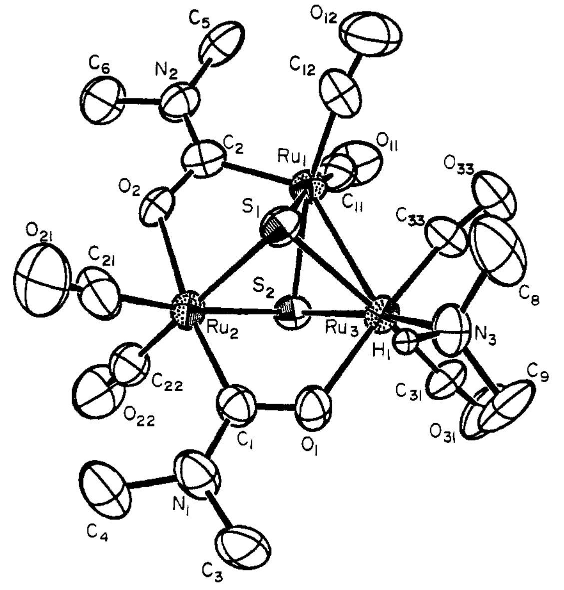

Figure 2. ORTEP diagram of $Ru_3(CO)_6(NHMe_2)(\mu\text{-}Me_2NC{=}O)(\mu_3\text{-}S)_2$ (**3**), showing 50% probability thermal ellipsoids. The hydrogen atom H(1) is shown with an artifically reduced thermal ellipsoid. The other hydrogen atoms are not shown.

two carbonyl ligands. C(33)–O(33) is leaning toward Ru(1), Ru(1)···C(33) = 2.72(2) Å, and could be described as a weak semibridging ligand. Structurally, all six methyl groups in the molecule are chemically inequivalent. Appropriately, six resonances were observed in the ^1H NMR spectrum in C_6D_6 solvent at 25 °C. The resonances at 1.94 and 1.86 ppm were doublets and can be assigned to the methyl groups on the amine ligand with coupling to the amine hydrogen atom. The resonances at 2.37 and 2.72 ppm were slightly broadened at 25 °C. At higher temperature they broadened further and coalesced at 56 °C. This pair of resonances can be assigned to the *N*-methyl groups on one of the bridging carbamoyl ligands, and the dynamic averaging can be attributed to the onset of rapid rotation about the C–N partial multiple bond. At 56 °C the resonances from the methyl groups in the other carbamoyl ligand were broadened. The temperature of coalescence for these resonances was not achieved, but it is fairly certain that the broadening is due to the onset of rapid rotation about the C–N multiple bond in the second carbamoyl ligand. Hindered rotation about the C–N bonds in carbamoyl ligands has been observed in certain mononuclear metal complexes.[9]

When compound **2** was allowed to react with CO (1 atm) for 5 h at 68 °C, the dimethylamine ligand was substituted by a CO ligand and yielded $Ru_3(CO)_8(\mu\text{-}Me_2NC{=}O)(\mu_3\text{-}S)_2(\mu\text{-}H)$ (**5**). The compound is spectroscopically very similar to the compound $Os_3(CO)_8(\mu\text{-}Me_2NC{=}O)(\mu_3\text{-}S)_2(\mu\text{-}H)$ obtained from the reaction of $Os_3(CO)_9(\mu_3\text{-}S)_2$ with Me_2NH and is therefore believed to be structurally similar.[2]

When compound **1** was allowed to react with limited amounts of Me_2NH, the reaction proceeded much more slowly. The reaction was followed both by IR and ^1H NMR spectroscopy. A similar sequence of transformations was observed by both techniques. An intermediate was formed first. It was spectroscopically very similar to the known compound $Fe_3(CO)_8(NHMe_2)(\mu_3\text{-}S)_2$ that was obtained from the reaction of $Fe_3(CO)_9(\mu_3\text{-}S)_2$ with Me_2NH.[2] Accordingly, this intermediate is formulated as $Ru_3(CO)_8(NHMe_2)(\mu_3\text{-}S)_2$ (**4**). Attempts to isolate **4** were unsuccessful. When more Me_2NH was added to the reaction, the IR absorptions and ^1H NMR resonances of **4** disappeared and those of **2** became prominent. With the addition of still more Me_2NH to the reaction, the IR absorptions and ^1H NMR resonances of **2** disappeared and those of **3** became prominent.

Discussion

The addition of amines to the carbon atom of carbonyl ligands in metal complexes has been well documented.[9] There are also several examples for the formation of bridging carbamoyl ligands from the reactions of secondary amines with $Ru_3(CO)_{12}$ and $Os_3(CO)_{12}$.[6,10] These reactions normally proceed in an addition/decarbonylation sequence. In our previous studies on the reactions of the sulfur-bridged clusters $M_3(CO)_9(\mu_3\text{-}S)_2$ (M = Fe, Os) with Me_2NH, we observed significant differences in the patterns of reactivity.[2] For the iron cluster there was no evidence of a reaction of amine at the carbonyl ligands. Instead, only a substitution reaction to yield $Fe_3(CO)_8(NHMe_2)(\mu_3\text{-}S)_2$ was observed. For the osmium cluster, addition at a carbonyl ligand to yield a bridging carbamoyl ligand was observed; however, decarbonylation did not occur. Instead, there was a cleavage of one of the metal–metal bonds. Similar transformations have been observed in the addition of methyllithium[11] and alcohols[12] to the pentanuclear carbido clusters $M_5(CO)_{15}(\mu_5\text{-}C)$ (M = Ru, Os).

Interestingly, the reaction of **1** with Me_2NH involves a combination of the reaction pathways observed for the iron and osmium homologues. Compound **2** contains a carbamoyl ligand bridging a nonbonded pair of metal atoms, but also contains a Me_2NH substituted for one of the carbonyl ligands. When reaction was performed with controlled additions of Me_2NH, it occurred at

---

(9) Angelici, R. J. *Acc. Chem. Res.* **1972**, *5*, 335.
(10) Azam, K. A.; Yin, C. C.; Deeming, A. J. *J. Chem. Soc., Dalton Trans.* **1978**, 1201.
(11) Cowie, A. G.; Johnson, B. F. G.; Lewis, J.; Nicholls, J. N.; Raithby, P. R.; Swanson, A. G. *J. Chem. Soc., Chem. Commun.* **1984**, 637.
(12) Braga, D.; Johnson, B. F. G.; Lewis, J.; McPartlin, M.; Nelson, W. J. H. *J. Chem. Soc. Chem. Commun.* **1982**, 966.

Scheme I. Reactions of Me_2NH with $M_3(CO)_9(\mu_3\text{-}S)_2$ Clusters

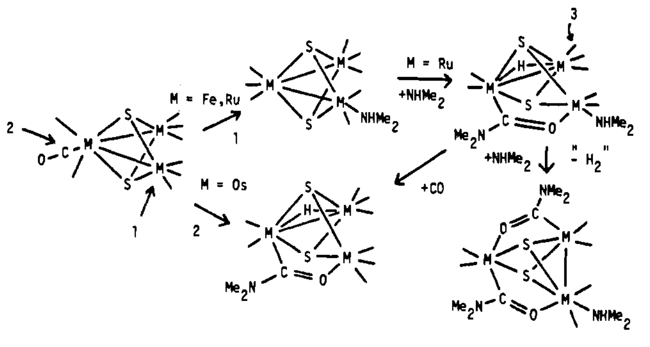

a rate that could be followed spectroscopically, and this has permitted the reaction sequence to be established. Before the formation of **2** occurred, an intermediate that was spectroscopically similar to $Fe_3(CO)_8(NHMe_2)(\mu_3\text{-}S)_2$ was formed. Accordingly, this intermediate has been formulated as **5** and this confirms that the first step in the formation of **2** is a CO substitution reaction on one of the two external metal atoms of cluster. See route 1 in Scheme I, which summarizes the reactions of all of the $M_3(CO)_9(\mu_3\text{-}S)_2$ clusters with Me_2NH. Only the osmium cluster reacts initially by route 2, which is attack upon a CO ligand in its first and only reaction step.

Unlike $Fe_3(CO)_8(NHMe_2)(\mu_3\text{-}S)_2$, **5** reacted with a second mole of Me_2NH by attack upon a CO ligand on the central metal atom of the cluster. This led to compound **2** by the formation of a bridging carbamoyl ligand. This reaction is believed to be analogous to the reaction of the sulfido–osmium cluster with Me_2NH. The mechanism of the shift of the hydrogen atom from the amine nitrogen atom to the cluster to become the bridging hydride ligand has not been established in these studies. Addition of CO to **2** yielded **4**, which would be the expected product from the addition of amine to CO ligand in **1**. We have not obtained any evidence for the formation of **4** by the latter route. The reason why **2** adds amine at a CO ligand and **1** does not is not clear, but the cleavage of the metal–metal bond could be an important factor. In the structure of $Fe_3(CO)_8(NHMe_2)(\mu_3\text{-}S)_2$, it was observed that the Fe–Fe bond, which included the amine-substituted iron atom, was much longer and, presumably, thus weaker than the other one. This is the bond that must be cleaved to form **2** from **5**, and if its cleavage has an important influence on the reaction rate, its weakening may produce a sufficient enhancement to permit the amine addition to proceed at a practical rate.

Compound **3** was formed from **2** by the addition of 1 equiv of Me_2NH. Attack is believed to occur at a CO ligand on the metal atom that contains three CO ligands (route 3). A second carbamoyl ligand is formed, and an equivalent of H_2 (not observed) must be eliminated. Mechanistically, it is believed that the hydride-bridged metal–metal bond is **2** is cleaved and the new carbamoyl ligand bridges that pair of metal atoms. As a consequence of the H_2 elimination a new metal–metal bond is formed, and all the metal atoms obey the 18-electron rule.

Acknowledgment. The research was supported by the National Science Foundation under Grant No. CHE-8416460. The AM-300 NMR spectrometer was purchased with funds from the National Science Foundation, Grant No. CHE-8411172.

Supplementary Material Available: Tables of anisotropic thermal parameters (*U* values) and hydrogen atom parameters (4 pages); tables of calculated and observed structure factors (34 pages). Ordering information is given on any current masthead page.

Contribution from the Departments of Chemistry, The Ohio State University,
Columbus, Ohio 43210, and The University of Warwick, Coventry CV4 7AL, U.K.

Synthesis and Characterization of a Lacunar Bis(isothiocyanato)cobalt(III) Cyclidene Complex: A Structural Model for Distal Steric Effects in Hemoproteins

Patricia J. Jackson, Colin Cairns, Wang-kan Lin, Nathaniel W. Alcock,* and Daryle H. Busch*

Received February 12, 1986

The synthesis and structural characterization of lacunar bis(isothiocyanato)cobalt(III) cyclidene complexes are presented. The effect of the restrictive lacuna on axial ligation is clearly seen from the results of the X-ray crystal structure determination of one of the complexes. Bis(isothiocyanato)(2,3,9,10,12,18-hexamethyl-3,9,13,17,20,24-hexaazabicyclo[9.7.7]pentacosa-1,10,12,17,19,24-hexaene-κ^4N)cobalt(III) hexafluorophosphate crystallizes in the orthorhombic space group $P2_12_12_1$, with a = 10.342 (4) Å, b = 14.857 (4) Å, and c = 21.933 (4) Å, and was solved by the heavy-atom method to R = 4.2%, R_w = 4.7%. Both axial isothiocyanate ligands are appreciably bent as a result of very different steric influences. The ligand within the lacuna is distorted by intramolecular van der Waals interactions with the pentamethylene bridge, while that coordinated at the less hindered axial site bends because of an intermolecular interaction with a PF_6^- counterion in the crystal lattice. A comparison is made with the analogous hexamethylene-bridged cobalt(III) complex, in which the counterion is a chloride, and the various factors that may give rise to such distortions are discussed.

Introduction

It has been over 30 years since St. George and Pauling observed[1] that the sterically demanding binding site of hemoglobin results in reduced equilibrium binding constants for a series of alkyl isocyanides in the order $K_{\text{EtNC}} > K_{i\text{-PrNC}} > K_{t\text{-BuNC}}$. This seminal work has since been quantified in thermodynamic and kinetic studies of both natural heme proteins and model porphyrin systems, in attempts to rationalize the relative affinities for hemoproteins of carbon monoxide and dioxygen. Carbon monoxide binds in a linear fashion in virtually all its iron(II) porphyrin complexes, while dioxygen invariably adopts a bent end-on configuration.[2,3] In contrast, x-ray structural studies on carbon monoxide complexes of heme proteins show distortion from this ideal linear structure, but the nature of the distortion has been obscured by the limitations of the studies. It has been suggested that the natural hemoproteins discriminate against CO, and other linear diatomic ligands, via a steric interaction between the bound ligand and a "distal" amino acid side chain. In human hemoglobin the closest candidate for such an interaction is histidine-E7, although Val-E11

---

* Authors to whom correspondence should be addressed: N.W.A., The University of Warwick; D.H.B., The Ohio State University.

[1] St. George, R. C.; Pauling, L. *Science (Washington, D.C.)* **1951**, *114*, 629.

[2] Phillips, S. E. V.; Schoenborn, B. P. *Nature (London)* **1981**, *292*, 81.

[3] Shaanan, B. *Nature* (London) **1982**, *296*, 683.